High Resolution Measurements of ^{12}C(γ, n) and the Implications for the (γ, N) Reaction Mechanism at Intermediate Energy

J. R. M. Annand, G. I. Crawford, P. D. Harty, J. C. McGeorge, and G. J. Miller

Department of Physics and Astronomy, University of Glasgow, Kelvin Laboratory, National Engineering Laboratory, East Kilbride G750QU, Scotland

B-E. Andersson, J-O. Adler, S. A. Bulychjev,* L. Isaksson, H. Ruijter, and B. Schrøder

Institute of Physics, University of Lund, Sölvegatan 14, S-223 62 Lund, Sweden

High resolution measurements of the reaction ^{12}C(γ, n) at $E_\gamma \sim 58$ MeV are presented. The distribution of strength to the resolved bound final states in ^{11}C is compared with that of ^{11}B obtained in previous analogous (γ, p) measurements and the implications for the theoretical description of (γ, N) reactions are discussed. These new results confirm the importance of two-nucleon effects in intermediate energy photon absorption and highlight inadequacies in state-of-the-art microscopic calculations of (γ, N) reactions.

The photon is an ideal probe of nuclear structure as the electromagnetic interaction is well understood and weak, so that the nucleus is only mildly perturbed. Thus in principle precise structure information may be extracted from photoreaction data, provided the photon absorption mechanism is known. In this work we have measured (γ, n) reaction cross sections in a bid to clarify (γ, N) reaction mechanisms in the energy region intermediate between nuclear collective resonances and nucleon resonances.

In the case of medium energy ($e, e'p$) reactions, which up to now have largely been performed in parallel kinematics at missing momenta $p_m \sim 200$ MeV/c, the exchanged virtual photon interacts predominantly by direct knockout (DKO) of a single nucleon. For (γ, N) reactions the transverse real photon has rather higher p_m, typically ~ 300 MeV/c for $E_\gamma \sim 60$ MeV, which tends to suppress DKO and there is strong evidence that photon absorption on two-nucleon ($2N$) currents is important. In particular early bremsstrahlung measurements showed that cross sections for the ^{16}O(γ, n_0) [1] and ^{16}O(γ, p_0) [2] reactions, which leave the $A = 15$ system in the hole, $\frac{1}{2}^-$ ground state, are of comparable magnitude although the photon interaction with the magnetic moment of the uncharged neutron is too weak to produce the observed (γ, n_0) cross section. Explanations based on microscopic [3] and phenomenological [4] models have been advanced. The former attempts to account for nucleon-nucleon (NN) correlation and meson exchange current effects, while the latter is a modified form of the quasideuteron (QD) model [5] where photon absorption on a correlated p-n pair is modeled using empirical D(γ, p)n cross sections and one of the ejected nucleons is reabsorbed, with the residual nucleus taking up the large missing momentum.

Since these early (γ, N) measurements were made the development of high duty factor electron accelerators has made the photon tagging technique [6] feasible, giving monochromatic photon sources of well known intensity. Used in conjunction with suitably high resolution hadron detectors, tagged photon (γ, p) experiments can now resolve discrete excited states in the $A - 1$ system. A relatively complete data set has been obtained for the ^{12}C(γ, p) reaction [7,8], with the most striking result being the strong excitation at ~ 7 MeV of a triplet of states in ^{11}B. These have large two hole, one particle (2h-1p) structural components, and are weakly excited in ^{12}C($e, e'p$) [9] which mainly probes single hole (1h) strength. The theoretical interpretation of (γ, N) reactions has also progressed. Microscopic theories [10,11], which use wave functions generated in the random phase approximation (RPA), are capable of calculating 1h transition matrix elements with exchange current effects implicitly included by the use of effective NN interactions and effective N masses. Recently they have been extended [12] to calculate 2h-1p transitions, explicitly accounting for one pion exchange currents (OPEC), but in this case using Hartree-Fock (HF) wave functions. These theories give a fair account of the data, but more measurements are required to assess the importance of various ingredients or omissions in the calculations. An investigation of the ^{12}C(γ, n) reaction provides the constraint that DKO should be virtually negligible so that the $2N$ absorption effects can be assessed with less ambiguity. This work reports the initial findings of such an experiment which is the first performed at intermediate energy to resolve excitations of the $\frac{3}{2}^-$ (0.00 MeV), $\frac{1}{2}^-$ (2.00 MeV), $\frac{3}{2}^-$ (4.80 MeV) states, and the unresolved triplet of states $\frac{1}{2}^+, \frac{7}{2}^-, \frac{5}{2}^+$ clustered around 6.5 MeV, thus providing experimental data of equivalent quality to those obtained in (γ, p). As such it represents a major advance on previous (γ, n) experiments, which are exceedingly few in number. The two published tagged photon measurements at intermediate energy [13,14] broadly
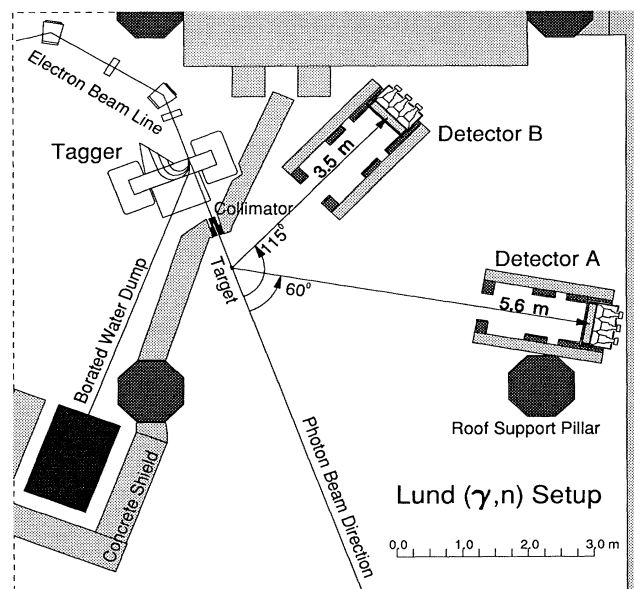
FIG. 1. Plan view of the photonuclear experimental area at MAXLAB. Neutron detectors are shown at high and medium resolution flight paths.

support the findings of the old bremsstrahlung measurements [1]. However, since discrete, $A - 1$ states were not resolved, these data provide only a limited degree of constraint on theoretical predictions.

The experiment, depicted in plan view in Fig. 1, was performed at the MAXLAB tagged photon facility [15], where a 75 MeV, 10 nA electron beam with $\sim 80\%$ duty factor produced bremsstrahlung in a thin Al radiator. This was tagged over the energy range 54.5–61.5 MeV with an energy resolution of ~ 0.3 MeV, to produce an overall flux of $\sim 10^6$ s^{-1} photons which impinged on a 8.5 g/cm^2 cylindrical graphite target. Neutron energy measurement was made using a time of flight (TOF) spectrometer which consisted of two $60 \times 60 \times 10$ cm NE213A liquid scintillators, each segmented as a 3×3 array. These were surrounded by borated paraffin and lead shielding, the former to attenuate low energy neutrons and the latter to attenuate photons and energetic neutrons. One detector was situated at long flight path for good energy resolution and the other at medium flight path for improved counting rate which was $\sim 3/(\text{h}\,\mu\text{b sr})$. Pulse shape analysis [16] distinguished neutron signals from electromagnetic background and charged particles were vetoed by thin plastic scintillators which encase the front and sides of the liquid cells. The time resolution of the tagger focal plane, TOF spectrometer combination was 0.8 ns FWHM. At a flight path of 6 m the expected energy resolution of 1 MeV FWHM is close to the 0.75 MeV achieved in state-of-the-art (γ, p). Absolute cross sections were calculated on the basis of the TOF and tagger focal plane detector counting rates. Corrections were made for tagging efficiency, neutron detection efficiency
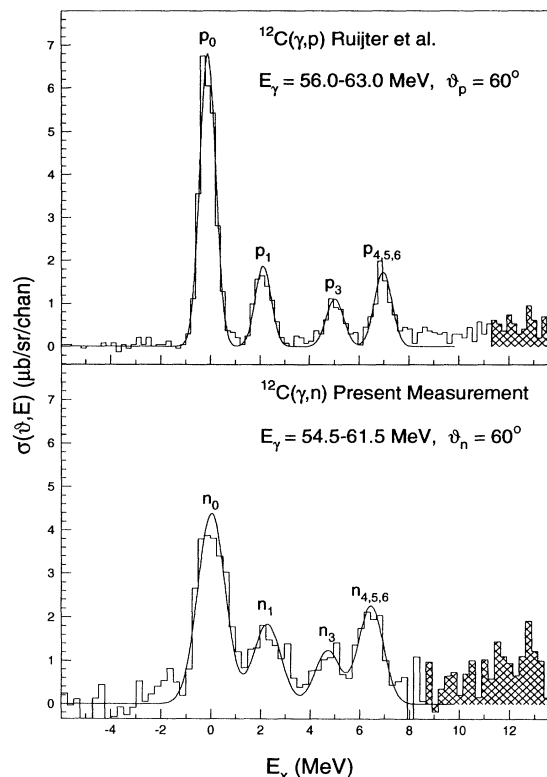

FIG. 2. Excitation energy spectra for the $A = 11$ nuclei produced in ^{12}C(γ, N) reactions.

of the liquid scintillators, and neutron attenuation in the target, air, front veto detectors, and the Al shell of the liquid scintillator. Tagging efficiency, the ratio of photons passing through the collimator (Fig. 1) to electrons detected in the tagger focal plane, was periodically measured with a 100% efficiency, lead glass Cherenkov, photon detector and the tagged photon flux was continuously monitored by an array of thin plastic scintillators. The average tagging efficiency was 21%. Measurements of D(γ, n) were also made with a D$_2$O target and checked against the relatively well known two-body photodisintegration cross section [17,18]. Peaks in the TOF spectra for D(γ, n) and ^{16}O(γ, n) also served to check the energy calibration of the spectrometer, as well as forming the basis of a parallel investigation of ^{16}O.

A spectrum of excitation energy, $E_x = E_\gamma - E_n - E_{A-1} + Q$, of the residual ^{11}C nucleus is presented in Fig. 2. Also shown is an analogous spectrum for ^{11}B [19] measured in ^{12}C(γ, p) at similar missing momentum. The hatched areas of the spectra indicate the regions of excitation which can be populated by ^{12}C(γ, np) which, since the second nucleon is undetected, produces a continuum. The ^{11}C spectrum exhibits prominent peaks from excitation of the $\frac{3}{2}^-$ (ground state), $\frac{1}{2}^-$ (2.00 MeV), $\frac{3}{2}^-$ (4.80 MeV), and the unresolved triplet centered around 6.5 MeV $\{\frac{1}{2}^+$ (6.34 MeV),
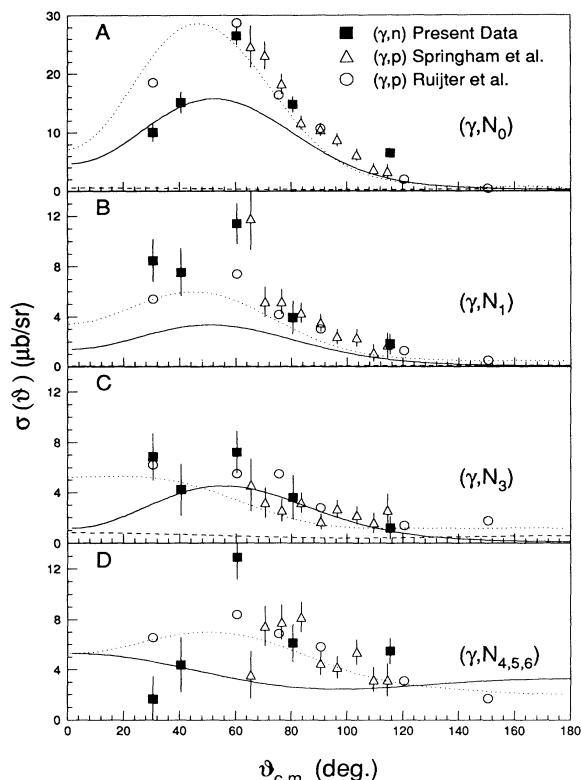
FIG. 3. Differential cross sections for $^{12}C(\gamma, N)$ reactions. Theoretical calculations of Ryckebusch are shown as a solid line (γ, n) and a dotted line (γ, p). Where the calculation is a coherent sum of RPA and HF + OPEC, the latter is shown for (γ, n) only as a dashed line.

$\frac{7}{2}^{-}$(6.48 MeV), $\frac{5}{2}^{+}$(6.91 MeV)}. These are precisely equivalent to the states of ^{11}B which are excited by (γ, p) and the distribution of strength appears to be very similar.

In Fig. 3 differential cross sections are plotted for each of the peaks observed in Fig. 2 and compared with the equivalent (γ, p) data [7,19]. The curves show the theoretical predictions of Ryckebusch [12,20] where RPA and HF + OPEC models are used to calculate 1h and 2h-1p components, respectively, of the $A = 11$ states. Apart from the triplet state [Fig. 3(d)], which is assumed to be pure 2h-1p, the full $[(\gamma, n)]$ and dotted $[(\gamma, p)]$ curves represent the coherent sum of RPA and HF + OPEC contributions. For (γ, p) the relative strengths of RPA and HF + OPEC can be seen in Ref. [12], while for (γ, n) the HF + OPEC contribution is given as a dashed curve in Figs. 3(a)–3(c). The (γ, n) and (γ, p) calculations are equivalent in that the same spectroscopic information has been used. Error bars on the present (γ, n) data reflect statistical uncertainties, which include uncertainties arising from the four Gaussian fitting procedure used to extract the peak areas. The values obtained are a factor ~ 1.7 higher than the equivalent cross sections of Harty et al.

[13], also measured using tagged photons, but with insufficient resolution to separate discrete states. As a check of the normalization, our measured $D(\gamma, n)$ differential cross sections at $E_\gamma = 54.5$–61.5 MeV were compared (Table I) with the measurements of Debevec et al. [17], extrapolated to $E_\gamma = 58$ MeV, and with the fit of Rossi et al. [18] to existing $D(\gamma, p)$ data sets, evaluated at 58 MeV. On the basis of these values the present $D(\gamma, n)$ measurements appear to be slightly low. However, a complete analysis of systematic errors still has to be performed and these are provisionally estimated at 20%.

In Fig. 3(a) the calculations follow the general trend in shape of the data, although the pronounced peak in the (γ, n_0) distribution is poorly reproduced. Similarly the theoretical curves of Fig. 3(b) predict (γ, p_1) tolerably well, but the (γ, n_1) cross sections are a factor 2–3 higher than the calculation. The (γ, n_3) and (γ, p_3) data of Fig. 3(c) are approximately equal. However, the calculations show rather different angular distributions, with the (γ, p) better reproducing the shape if not the magnitude of the data. In Fig. 3(d) theory and data are in reasonable accord for (γ, p). Here the theoretical curves are pure HF + OPEC, but again the (γ, n) shape is quite different from the (γ, p) and is at variance with the present data, failing to reproduce the steep plunge in cross section at forward angles. It would be instructive to have more (γ, p) data in this kinematic domain to check if this is a general feature of (γ, N). For the (γ, n) calculations the spectroscopic strengths of the individual states of the triplet have been assumed the same as for (γ, p) [12]. Each state has a rather different angular distribution, but it is unlikely that any adjustment of relative strengths will produce a fit to the data.

The most striking feature of the present data is the overall close similarity of (γ, n) and (γ, p) cross sections, which can be envisaged quite naturally in the phenomenological QD model and strongly suggests that photon absorption on NN exchange currents is an important mechanism in the intermediate energy region. State-of-the-art microscopic calculations, which reproduce (γ, p) with reasonable accuracy, agree rather poorly with the present (γ, n) measurements. The RPA calculations (1h components of $A = 11$ states) use a one-body electromagnetic transition operator, but exchange effects are implicitly included through the use of effective, Skyrme-type, NN interactions and effective N masses. Thus it is nontrivial to distinguish effects which might conveniently be labeled DKO, NN exchange, or final state interaction. The HF+OPEC calculations explicitly include "seagull"

TABLE I. Differential cross sections in μb/sr for $D + \gamma \to p + n$ at $E_\gamma = 58$ MeV.

$\theta_{c.m.}$	Present measurement	Ref. [17]	Ref. [18]
34.0	8.0±1.5	9.2	10.2
87.0	10.4±2.3	14.3	13.5

and "pion in flight" diagrams, but still fail to describe the $(\gamma, n_{4,5,6})$ cross section. Therefore it is clear that the present measurements have revealed inadequacies in the current microscopic (γ, N) theory. These will be further explored with (γ, p) and (γ, n) data on ^{16}O which are presently under analysis. The $A = 15$ negative parity states are pure 1h while those of positive parity are predominantly 2h-1p, so that a possible source of uncertainty in the calculations, regarding the structure of the $A = 11$ states, is removed.

* Permanent address: ITEP, Moscow 117259, Russia.

[1] H. Göringer, B. Schoch, and G. Lührs, Nucl. Phys. A384, 414 (1982).

[2] D. J. S. Findlay and R. O. Owens, Nucl. Phys. A292, 53 (1977).

[3] M. Gari and H. Hebach, Phys. Rep. 72, 1 (1981).

[4] B. Schoch, Phys. Rev. Lett. 41, 80 (1978).

[5] J. S. Levinger, Phys. Rev. 84, 43 (1951).

[6] J. D. Kellie, I. Anthony, S. J. Hall, I. J. D. MacGregor, A. MacPherson, P. J. Thorley, S. L. Wan, and F. Zettl, Nucl. Instrum. Methods Phys. Res., Sect. A 241, 153 (1985).

[7] S. V. Springham, D. Branford, T. Davinson, A. C. Shotter, J. Yorkston, J. C. McGeorge, J. D. Kellie, S. J. Hall,

R. Beck, P. Jennewein, and B. Schoch, Nucl. Phys. A517, 93 (1990).

[8] L. Van Hoorebeke, D. Ryckbosch, R. Van de Vyver, H. Ferdinande, D. Nilsson, J-O. Adler, B-E. Andersson, K. I. Blomqvist, L. Isaksson, A. Sandell, B. Schrøder, and K. Ziakas, Phys. Rev. C 42, R1179 (1990).

[9] G. Van Der Steenhoven, H. P. Blok, E. Jans, M. De Jong, L. Lapikas, E. N. M. Quint, and P. K. A. De Witt Huberts, Nucl. Phys. A480, 547 (1988).

[10] M. Cavatino, M. Maragoni, and A. M. Saruis, Nucl. Phys. A422, 237 (1984).

[11] J. Ryckebusch, M. Waroquier, K. Heyde, J. Moreau, and D. Ryckbosch, Nucl. Phys. A476, 237 (1988).

[12] J. Ryckebusch, K. Heyde, L. Machenil, D. Ryckbosch, M. Vanderhaeghen, and M. Waroquier, Phys. Rev. C 46, R829 (1992).

[13] P. D. Harty, M. N. Thompson, G. J. O'Keefe, R. P. Rassool, K. Mori, Y. Fujii, T. Suda, I. Nomura, O. Konno, T. Terasawa, and Y. Torizuka, Phys. Rev. C 37, 13 (1988).

[14] J. A. Eden, G. J. O'Keefe, R .P .Rassool, D. J. McLean, M. N. Thompson, T. Suda, I. Nomura, J. Yokokawa, O. Konno, T. Terasawa, and Y. Torizuka, Phys. Rev. C 44, 753 (1991).

[15] J-O. Adler, B-E. Andersson, K. I. Blomqvist, B. Forkman, K. Hansen, L. Isaksson, K. Lindgren, D. Nilsson, A. Sandell, B. Schrøder, and K. Ziakas, Nucl. Instrum. Methods Phys. Res., Sect. A 294, 15 (1990).

[16] J. R. M. Annand, Nucl. Instrum. Methods Phys. Res., Sect. A 262, 371 (1987).

[17] P. T. Debevec, P. D. Harty, J. E. Knott, D. A. Jenkins, and R. T. Jones, Phys. Rev. C 45, 904 (1992).

[18] P. Rossi, E. De Sanctis, P. Levi Sandri, N. Bianchi, C. Guaraldo, V. Lucherini, V. Muccifora, E. Polli, A. R. Reolon, and G. M. Urciuoli, Phys. Rev. C 40, 2412 (1989).

[19] H. Ruijter (private communication).

[20] J. Ryckebusch (private communication).